JOURNAL OF GEOPHYSICAL RESEARCH, VOL. 114, A02218, doi:10.1029/2008JA013079, 2009

FAST observations of downward current regions: Effect of magnetospheric conditions on the parallel potential drop

K.-J. Hwang,[1] K. A. Lynch,[2] D. L. Newman,[3] and C. W. Carlson[4]

Received 6 February 2008; revised 31 October 2008; accepted 9 December 2008; published 21 February 2009.

[1] The effects of background plasma sheet boundary conditions on the downward current region potential structures are investigated using FAST observations of both ionospheric and plasma sheet populations. Precipitating plasma sheet electrons are observed to partially control the magnitude of the potential drop consistent with theories of charge-neutrality requirements throughout ionospheric and magnetospheric regions. This leads to a new empirical model of a downward current region (DCR) current-voltage relation for U-shaped events. Hot plasma sheet ions are observed to play an important role in reducing the variability of the potential drop, possibly by acting as a sink or buffer for free energy caused by the resulting energetic upward electron beams. The statistical studies of boundary conditions in the auroral downward current region in this and our companion paper show that both ionospheric and magnetospheric conditions appear to regulate the DCR potential structures observed at FAST altitudes. The initiation of downward current region potentials seems to be influenced mainly by low-altitude ionospheric conditions. Once the U-shaped potential structure is formed, the effects of the ionospheric influences may be relaxed and modulated by effects from magnetospheric conditions.

Citation: Hwang, K.-J., K. A. Lynch, D. L. Newman, and C. W. Carlson (2009), FAST observations of downward current regions: Effect of magnetospheric conditions on the parallel potential drop, *J. Geophys. Res.*, *114*, A02218, doi:10.1029/2008JA013079.

1. Introduction

[2] FAST (Fast Auroral Snapshot) satellite observations illustrate the positive-potential structure responsible for particle acceleration in the auroral downward current region (DCR) by the signatures of diverging DC electric fields perpendicular to the ambient magnetic field ($\mathbf{E}_\perp$) with upgoing electron fluxes [*Carlson et al.*, 1998] and direct measurements of localized parallel electric fields ($\mathbf{E}_\parallel$) [*Ergun*, 2003; *Andersson*, 2002].

[3] *Hwang et al.* [2006a, 2006b] show that these DCR potential structures often have a more varied and complicated structure than an idealized longitudinally elongated sheetlike arc. This has implications for models of the formation and evolution of DCR potential structures corresponding to their coupling to the ionosphere. In previous manuscripts [*Hwang et al.*, 2006a, 2006b] we have shown that sheetlike DCR structures correspond to composite (ionospheric plus U-shaped) DC electric fields, while curved DCR structures correspond to dominantly U-shaped DC electric fields.

[4] According to the proposed evolutionary scenario, during the earliest stages of the formation of the parallel potential, U-shaped potentials nested within ionospherically defined structures (composite structures) resist being corrugated by Kelvin-Helmholtz instabilities, and therefore maintain the initially defined straight arc form. At a later time, after the relaxation of the ionospheric fields and widening of the current channel [*Marklund et al.*, 2001], the U-shaped potential contours may decouple from the lower ionosphere and form folds or filaments which are observed as curved structures by FAST. At this stage, being free from the ionospheric constraints, a consistent relation between downward current density and the magnitude of the U-shaped potential drop (called current-voltage or IV relation) can be expected, though the structure itself may widen in order to acquire more charge carriers.

[5] Figure 1 illustrates this proposed evolution of the DCR potential structure. Ionospheric fields are represented as thin green lines, and U-shaped as thick green lines. Representative FAST trajectories which pass across the flux tube are shown as violet dashed arrows. Upgoing ionospheric electrons are shown with red arrows, and precipitating plasma sheet populations are shown as dotted red arrows.

[6] In our companion paper [*Hwang et al.*, 2009], we show how parallel signatures of composite and U-shaped

[1]NASA Goddard Space Flight Center, Greenbelt, Maryland, USA.
[2]Department of Physics and Astronomy, Dartmouth College, Hanover, New Hampshire, USA.
[3]Center for Integrated Plasma Studies, University of Colorado, Boulder, Colorado, USA.
[4]Space Sciences Laboratory, University of California, Berkeley, California, USA.

0148-0227/09/2008JA013079$09.00

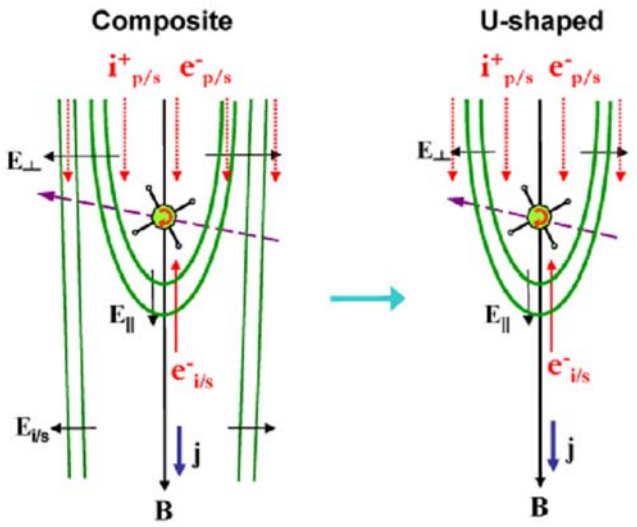

Figure 1. A proposed evolution of the auroral downward current region potential structure in the work of *Hwang et al.* [2006b]. Ionospheric fields are represented as a thin green line, and U-shaped, a thick green line. Representative FAST trajectories are shown as violet dashed arrows, upgoing ionospheric electrons as a red arrow, and precipitating plasma sheet populations as dotted red lines.

structures are affected by the coupling/decoupling to the lower ionosphere, and demonstrate that their different parallel signatures support the proposed evolutionary scenario of *Hwang et al.* [2006b]. That study concludes by questioning what role ionospheric boundary conditions play in determining signatures of the high-potential region of the DCR potential drop (i.e., at altitudes above the potential drop). In this paper, we continue investigating these environmental effects by focusing on the effects of background plasma sheet populations on the DCR potential structures and temporal signatures. The relationship of these potential structures to their background environment is important for understanding magnetosphere-ionosphere (MI) coupling and DCR current-voltage relations.

[7] Recently, efforts to find how magnetospheric electrons affect the DCR parallel potentials have been reported by L. Andersson et al. (Influence of supra-thermal background electrons on strong double layers: Observations, submitted to Physics of Plasmas, 2007) and D. Newman et al. (Influence of supra-thermal background electrons on strong double layers: Numerical simulations, submitted to *Physics of Plasmas*, 2007). Observations of different variabilities of upgoing electron fluxes in the downward current region indicate that events where the electron characteristic energy remains relatively constant are often observed together with a suprathermal isotropic electron "halo," a precipitating plasma sheet electron population of energies greater than 100 eV. Newman et al.'s (submitted manuscript, 2007) simulation related to this study shows that the evolution of the turbulent region into either a turbulent state or a laminar state depends on magnetospheric conditions, with the presence of halo electrons enhancing the probability of a laminar structure.

[8] Motivated by these studies, we use FAST statistical studies to investigate how magnetospheric conditions, as indicated by observations of plasma sheet populations, can be seen to control aspects of DCR potential-structure behavior. In this paper, we consider both plasma sheet ions and electrons ('halo' electrons) for investigations of magnetospheric boundary effects and observed current-voltage relations. The purpose of this paper is to determine how these plasma sheet populations affect the DCR potential structures and their fluctuations, and how they contribute to the DCR current-voltage (IV) relation for U-shaped events, and ultimately to complete our study about the roles that ionospheric and magnetospheric boundary conditions play in magnetosphere-ionosphere (MI) coupling in the auroral downward current region.

[9] In section 2, we present the effects of background plasma sheet hot ions on the DCR potential structures. In section 3, we analyze the effects of precipitating plasma sheet electrons (halo electrons), and propose a new empirical model of a DCR current-voltage relation. Discussion and summary are given in sections 4 and 5. The statistical analysis used to compare composite to U-shaped events in this paper is based on the same data set used in our companion paper [*Hwang et al.*, 2009]. This data set comprises 64 DCR events where strong (>100 mV/m) $E_\perp$ events occur, taken from 50 FAST orbits at altitudes from 2500 km to 4100 km. Events are from either the prenoon dayside or near-midnight local time regions, and the data are comprised of high time resolution (sampling rate of 16 msec) particle burst data. In addition, 55 further U-shaped events are collected abiding by the same criteria for sampling data, from 43 FAST orbits from orbits 1900 to 4100, in order to enhance the statistical evidence for the effects of plasma sheet populations on the stability and magnitude of DCR potential drops.

2. Effects of Hot Ions of Plasma Sheet Origin on the Downward Current Potential Structure

[10] We begin with the occurrence of hot plasma sheet ions with energy of a keV or greater, during both U-shaped and composite events. Figure 2 illustrates typical auroral downward current region features. Figure 2b shows a downgoing electron energy spectrogram, where the background populations of energies about 100 eV before 3 February 1997/19:29:18 UT, or around 1 keV after 3 February 1997/19:29:21 UT, represent plasma sheet 'halo' electrons. Correspondingly, hot plasma sheet ions are observed with energies of one or a few keV before 3 February 1997/19:29:18 UT, and several to 10 keV after 3 February 1997/19:29:21 UT in the ion energy spectrogram (Figure 2d). We define weak plasma sheet ion events as events where the plasma sheet ion energy fluxes are less than 10^5 eV/cm^2-s-sr-eV. Strong hot-ion events are those with hot ion energy fluxes greater than 10^5 eV/cm^2-s-sr-eV. The statistics of the events in our study show that plasma sheet hot ions, either intense or weak, are commonly found in the downward current region. There is no distinction in occurrence between the U-shaped and composite classifications, except that stronger hot-ion events (often dominated by higher fluxes rather than higher energies) are observed with U-shaped events.

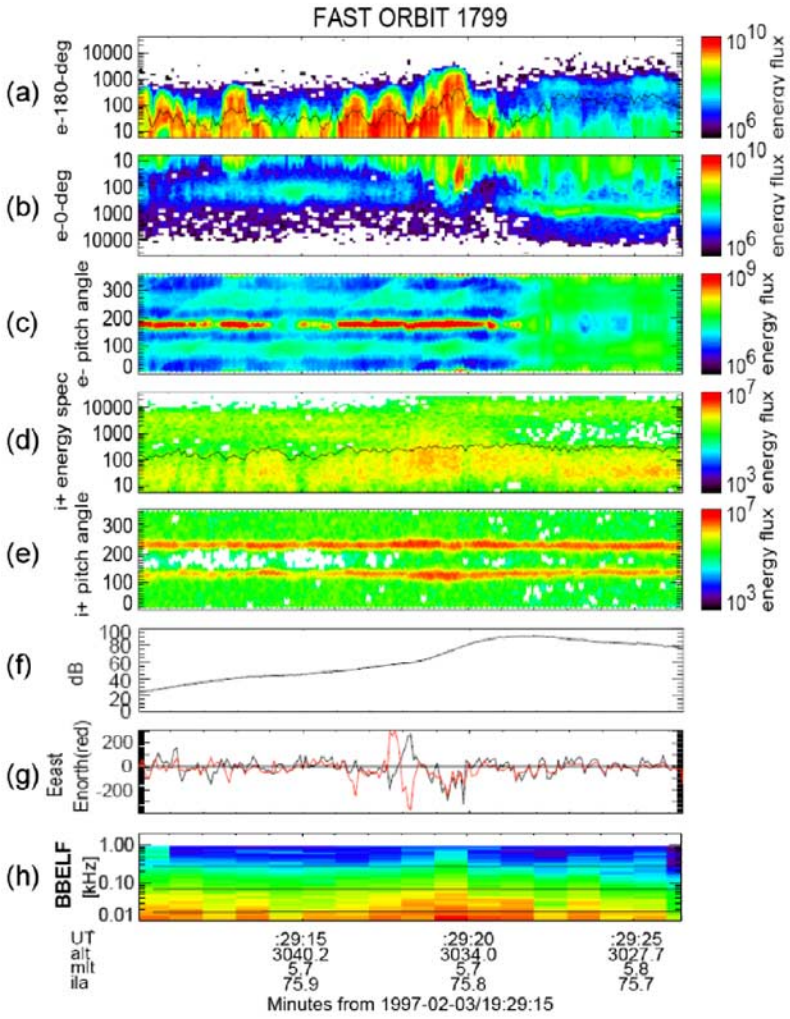

Figure 2. A FAST DCR crossing: (a) upgoing electron spectrogram, (b) downgoing electron spectrogram, (c) electron pitch angle distribution, (d) ion energy spectrogram of all pitch angles (thin black line represents ion characteristic energy defined as the energy flux divided by the number flux), (e) ion pitch angle distribution, (f) the magnetic field fluctuation, (g) two components of $\mathbf{E}_\perp$, east-west component of $\mathbf{E}_\perp$ in black, north-south component in red, and (h) BBELF wave electric field spectrogram.

[11] Next we consider a quantitative relationship between plasma sheet hot ions and DCR potential-drop behavior. Figure 3 shows the relationship between hot ion pressure and the variability of the magnitude of potential drop. For this comparison, the upgoing electron characteristic energy (defined as the energy flux divided by the number flux, ϵ_{ce}) is used as a measure of the potential drop magnitude. In our statistics, ϵ_{ce} extends from 17 eV to 1400 eV. The variability of the potential drop can be appropriately represented by the relative standard deviation of ϵ_{ce}, which we define as the standard deviation of ϵ_{ce} normalized by its mean value during a very short time (a few seconds of FAST crossing) around the most intense electron upfluxes.

[12] Uncertainties in our data (shown in Figure 3, and hereafter) are calculated from those of the sensors' geometric factor, which are found to vary <20% [*McFadden et al.*, 1999]. Other sources of data contamination are minor for the selected energy and pitch angle ranges for each of our data sets. The geometry-factor-derived uncertainties for a few representative points in each plot are marked as error bars.

[13] There is a clear decrease in variability with increasing hot-ion pressure above about 1500 eV/cm^3 (marked in green, where R, correlation coefficient = 0.787). The off-trend data points below 1500 eV/cm^3 represent a significant contribution to the ion pressure moment from ionospheric ions instead of dominant plasma sheet ions. In these cases, ions of plasma sheet and ionospheric origin are merged in the ion-energy spectrogram, and these cases are thus excluded from the correlation. (The lower limit of 1500 eV/cm^3 is determined by the typical, ionospheric-plasma density at FAST altitudes of about 4000 km, and the typical energy level where the two populations are often observed to be merged.)

[14] Since this variability is composed from the multiplication of $1/\epsilon_{ce}$ with the standard deviation of ϵ_{ce}, we examine

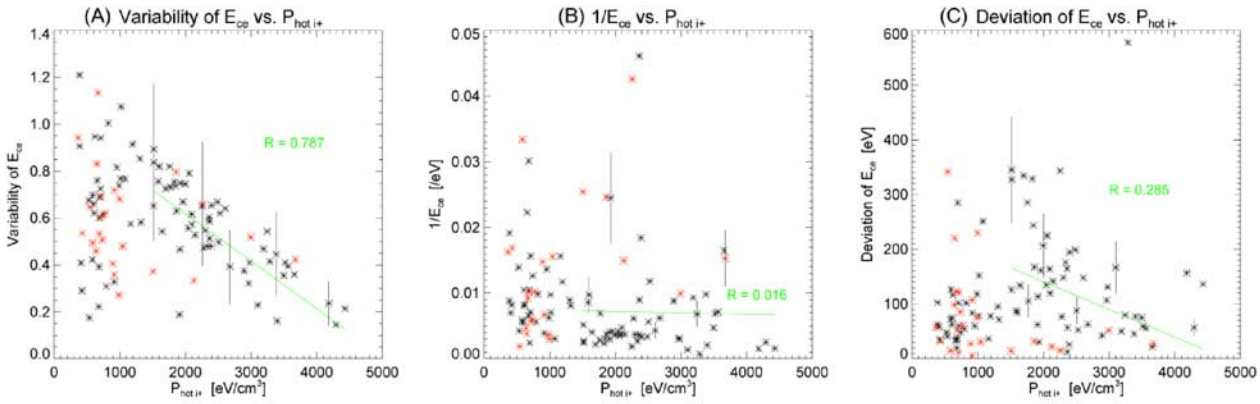

Figure 3. (a) The variability of potential drop, $\delta\epsilon_{ce}/\epsilon_{ce}$ as a function of hot ion pressure, (b) the reciprocal of the potential drop as a function of hot ion pressure, and (c) the standard deviation of the potential drop as a function of hot ion pressure. Black dots correspond to U-shaped events, red to composite. Uncertainties in these data are derived from those of the sensors' geometric factors, and representative error bars are shown.

separately the correlation to each of these. Figures 3b and 3c show the relationship of hot ion pressure to the reciprocal of ϵ_{ce}, and to the standard deviation of ϵ_{ce}, respectively. There is only a weak (R = 0.285) tendency that the higher ion pressure events have lower (absolute) deviation of ϵ_{ce} and there is no correlation (R = 0.016) between hot ion pressure and the average ϵ_{ce} for high ion pressure data greater than 1500 eV/cm^3. Thus, both confirm that the strong anticorrelation of Figure 3a truly shows a dependence on variability, not simply the inverse energy or deviation of ϵ_{ce}.

[15] These statistics show that when high-pressure plasma sheet ions are present, less variable downward potential structures are observed. This implies that hot ions play an important role in reducing the variability of the potential drop.

3. Effects of Halo Electrons on the Downward Current Region Potential Structure

[16] In this section, we consider the effect of a suprathermal plasma sheet electron population ("halo") of an energy of greater than about 100 eV. We define "halo events" as those that have a halo electron population with an energy flux of 10^8 eV/cm^2-s-sr-eV or higher. Our initial 64-sample statistics, as shown in Figure 4, show that "no halo" events dominate for composite events while halo events dominate for U-shaped events.

[17] This is consistent with the Newman et al. (submitted manuscript, 2007) and Andersson et al. (submitted manuscript, 2007) findings that halo events enhance the probability of a laminar state of the potential drop, since our evolutionary scenario expects that composite events (no halo) precede the development of U-shaped (halo) ones, and that the latter can be expected to be more laminar and less intermittent.

[18] Although our qualitative comparison for the halo occurrence agrees with the implications from these previous studies, our quantitative result is, however, not completely consistent with the studies by Andersson et al. (submitted manuscript, 2007) and Newman et al. (submitted manuscript, 2007). Unlike their conclusion, our statistics do not show a distinct relation between the halo energy or pressure, and the variability of ϵ_{ce}. Instead, we have seen that the stability of the potential drop is mainly controlled by hot plasma sheet ions (Figure 3) as demonstrated in section 2.

[19] We do see that halo electrons and hot ions are positively, though weakly, correlated. Figure 5 shows the statistics of the relationship between halo electron and hot ion pressure. All data points within each event (both U-shaped and composite) are plotted as groups of dots, with 18 selected events overplotted in various colors. The highest ion-energy events (where data values exceed the upper energy range of FAST ion detector) are excluded. U-shaped

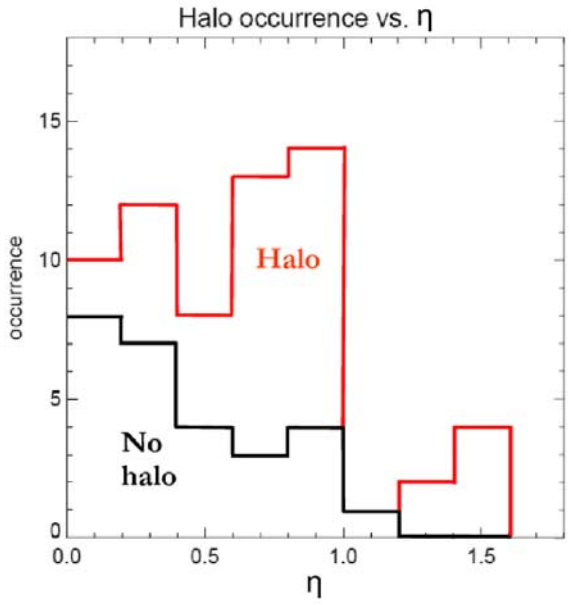

Figure 4. Histogram of the occurrence of halo events as a function of η. Small η (less than 0.5) represents composite events, large η (greater than 0.5) U-shaped ones. Details of η parameterization are given by *Hwang et al.* [2006b].

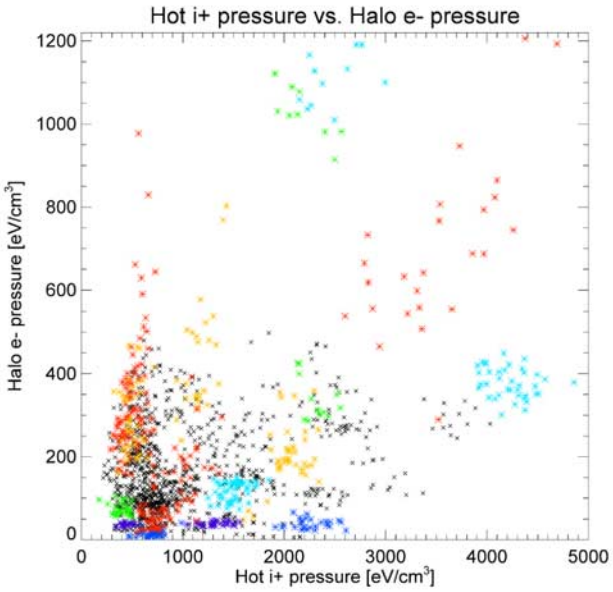

Figure 5. A scatterplot of halo electron pressure and hot plasma sheet ion pressure. Data from 18 selected orbits are marked as several colors as examples. Events for which the ion energy values exceed the upper energy range of the FAST ion detector are excluded.

events show a better proportionality between hot ion and halo electron pressures than do composite events (the eight events marked as green, blue, and sky-blue dots are composite events), and in general there is a linear tendency between halo electron pressures and hot plasma sheet ion pressures. This correspondence between the two magnetospheric populations can make it appear that halo electrons instead of hot ions regulate the fluctuations of the potential magnitudes.

[20] Finally, Figure 6 shows the relationship between halo electron pressure and electron characteristic energy (a proxy for the magnitude of parallel potential drop) for eight individual events selected from our U-shaped statistics. Time series data points during the FAST crossing for each of these eight events are represented as dots in each panel. A positive correlation between halo pressure and the magnitude of potential drop within each event is distinctly noticeable, but the slope and intercept vary from event to event. *Temerin and Carlson* [1998] predict that magnetospheric electrons should control $\mathbf{E}_{\|}$ for a given parallel current density, and our result leads to a DCR current-voltage relation where magnetospheric electrons play a role, as investigated in the following section.

4. Current-Voltage Relations

[21] Having seen that most of the U-shaped events show a good correlation between halo pressure and $\epsilon_{\mathbf{ce}}$ within each event, we approach the question of the downward current region current-voltage relation including the influence of magnetospheric electrons for the U-shaped events.

[22] Figure 7 shows $\epsilon_{\mathbf{ce}}$ as a function of the measured downward field-aligned current $\mathbf{J}_{e\|}$ from eight events among the 80 U-shaped examples. The field-aligned current is calculated from the electron drift moment using an energy range of 10 eV to 10 keV. Some events show a positive correlation, and some do not. It should be noted that the electron moment calculation misses electrons under 10 eV and above 10 keV, so if a significant downward current is carried by these electrons, the current density will be underestimated [*Lynch et al.*, 2002]. These relationships are no clearer when the downward current density derived from the magnetometer is used rather than from electron data, probably because the magnetometer derivation has other problems such as a sheetlikeness assumption.

[23] Next we bring in the effects of the halo pressure. For this step, each event is represented by a single averaged value of $\mathbf{J}_{e\|}$, halo pressure $\mathbf{P_{halo}}$, and characteristic energy. Figure 8 shows $\epsilon_{\mathbf{ce}}$ (in y axis) for all 80 U-shaped events as a function of the halo pressure $\mathbf{P_{halo}}$ (Figure 8a) and the downward current density measured from electrons $\mathbf{J_{e\|}}$ (Figure 8b), a combined parameter of these two, $\mathbf{J_{e\|}^2} \times \mathbf{P_{halo}^{2.91}}$ (Figure 8c), the same plot as Figure 8c but with the x axis in log scale (Figure 8d), and the analytic net potential drop along the downward current region flux tube based on *Cran-McGreehin and Wright* [2005a, 2005b] (Figure 8e).

[24] When the current density and halo pressure are combined in the formula as shown in Figures 8c or 8d, the data points converge to a linearly fitted function. (Note that the least squares fits in Figures 8c or 8d and Figure 8e were made by minimizing the sum of the horizontal distances between each data point and the fitted line, since in these panels the dominant error source is in the x axis parameter.) Red lines in each panel are the results of this fitting when all 80 U-shaped events are considered, including one red data point which shows significant Alfvénic activity (non-quasi-static behavior) compared to the other events. The blue fitted line shows the result when the red data point is excluded from the fitting. The correlation coefficient, R is 0.691 (Figure 8a), 0.859 for red (Figure 8c), and 0.716 (Figure 8a), 0.867 for blue (Figure 8c). For both fits, Figure 8c of the combined parameters shows a better correlation than does Figure 8a. The squared power dependence for the current density corresponds to the analytic results of *Cran-McGreehin and Wright* [2005a, 2005b] with low power terms suppressed in their model. The power 2.91 for the halo pressure term is empirically determined by maximizing the correlation between $\epsilon_{\mathbf{ce}}$ and $\mathbf{J_{e\|}^2} \times \mathbf{P_{halo}^n}$, where n is a variable to be determined, under the assumption of the squared power for the current density.

[25] For a closer comparison of the observed potential drop ($\epsilon_{\mathbf{ce}}$) to the analytic potential drop proposed by *Cran-McGreehin and Wright* [2005a, 2005b], a few assumptions were made in order to derive the analytic potential drop: the electron density in the F region is assumed 10^5 cm^{-3}, the density in a distant reference point in the magnetosphere is taken as 0.1 cm^{-3}, the ion scale height as 100 km, and c_p as 4.671×10^5 from Table 1 in the work of *Cran-McGreehin and Wright* [2005a, 2005b]. Dimensionless, analytic values of the potential drop are obtained from the measured data for $J_{e\|}$, halo density and pressure, and from equation (31) in the work of *Cran-McGreehin and Wright* [2005a, 2005b].

[26] A fairly good correlation is shown between the measured $\epsilon_{\mathbf{ce}}$ and the analytically induced potential drop

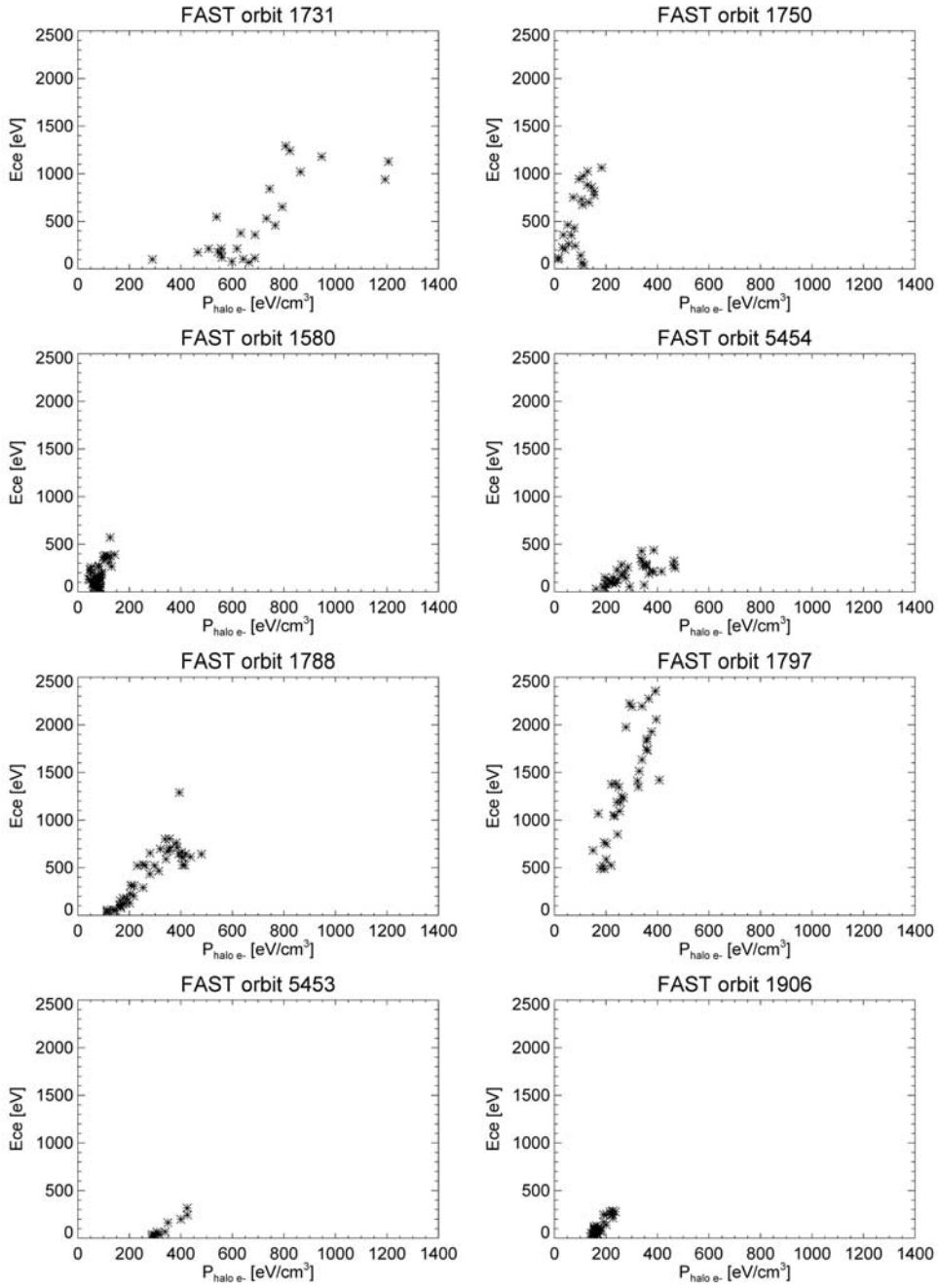

Figure 6. The magnitude of potential drop, estimated from the upgoing electron characteristic energy, as a function of halo pressure. Eight different events are shown.

with the correlation coefficient of 0.649 for red, and 0.659 for blue. Correlations are rather weaker than those of our empirical model in Figure 8c. The most noticeable difference between the empirical and analytic models is that the measurements correlate the potential drop to the magnetospheric electron pressure. *Cran-McGreehin and Wright* [2005a, 2005b], or *Temerin and Carlson* [1998] (from which the studies of *Cran-McGreehin and Wright* [2005a, 2005b] had been motivated) correlate it to magnetospheric electron temperature and density separately, and found a positive correlation with temperature and negative correlation with density.

[27] The difference between the empirical (Figures 8c or 8d) and analytic (Figure 8e) models might be explained by the assumptions made for the analytic value and the local measurements of FAST. For instance, $\epsilon_{\mathbf{ce}}$ measured by FAST would not represent the net parallel potential along the acceleration region of a DCR flux tube, but rather indicates a fraction of it, measuring the potential drop up to the FAST altitude. Our results imply that if the DCR parallel potential drop is distributed along the flux tube extending several thousand km in altitude, the potential drop magnitude near the ionosphere up to FAST altitude is significantly controlled by halo pressure, and the combined

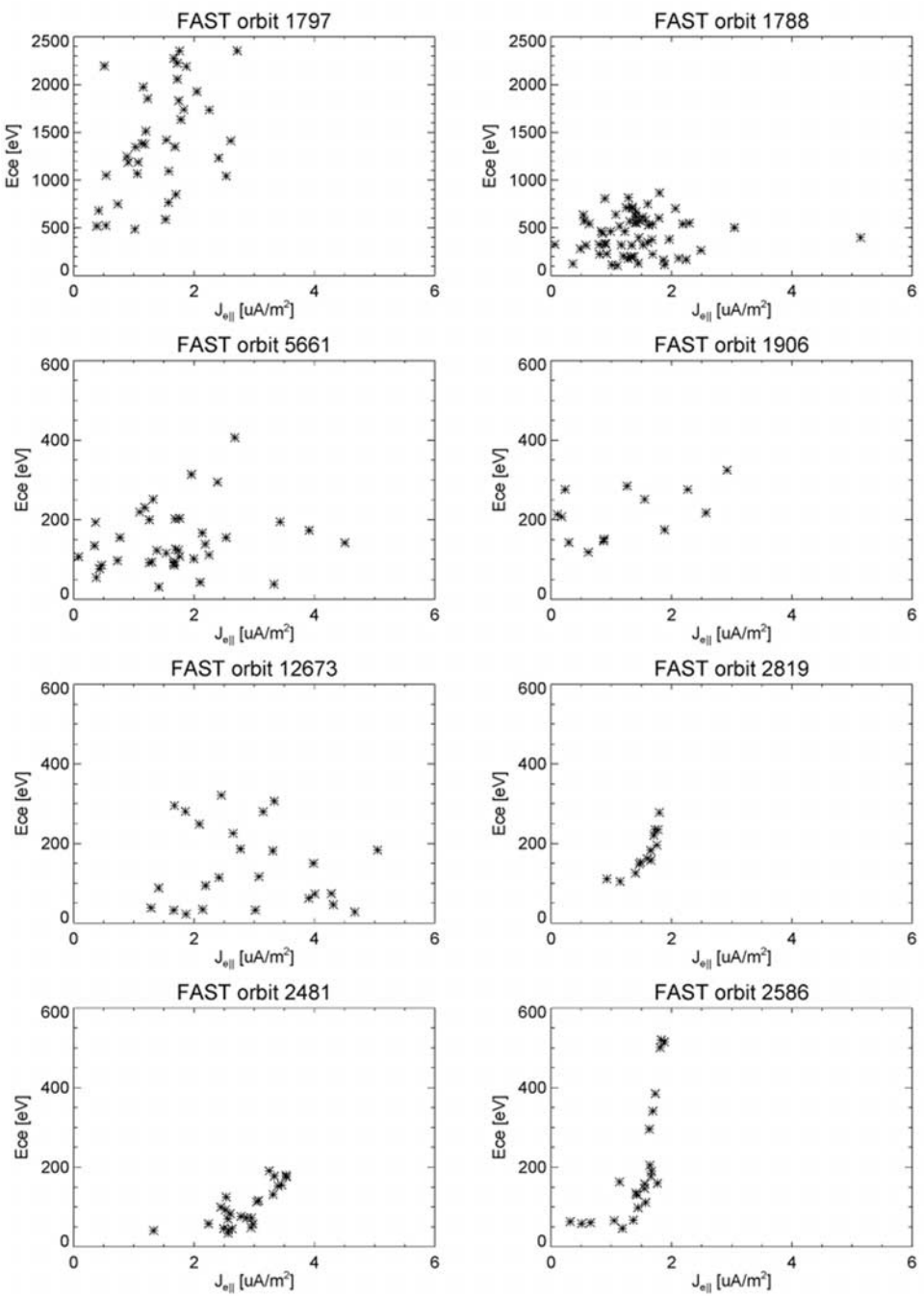

Figure 7. The magnitude of the potential drop as a function of the measured downward field-aligned current from electron moments (detailed in text) for eight U-shaped event examples. Each panel corresponds to one event.

parameter of downward current density and halo pressure should be taken into account in a DCR current-voltage relation.

5. Discussion

[28] The observation of along-flux-tube particle fluxes of ionospheric upgoing electrons and plasma sheet electron and ion populations at FAST DCR crossings suggests the importance of the effects of background magnetospheric conditions on the downward current region potential structures. Plasma sheet halo electrons and hot ions are found to play roles in the current-voltage relation of the downward current region, and in the variability of the parallel potential drop.

[29] Recently the presence of halo electrons was found to contribute to stabilization of the downward potential drop or double layer structures, maintaining its apparently stable state (Andersson et al., submitted manuscript, 2007; Newman et al., submitted manuscript, 2007).

[30] Our statistics show that halo events are dominantly found in U-shaped events. This result seems to be consistent

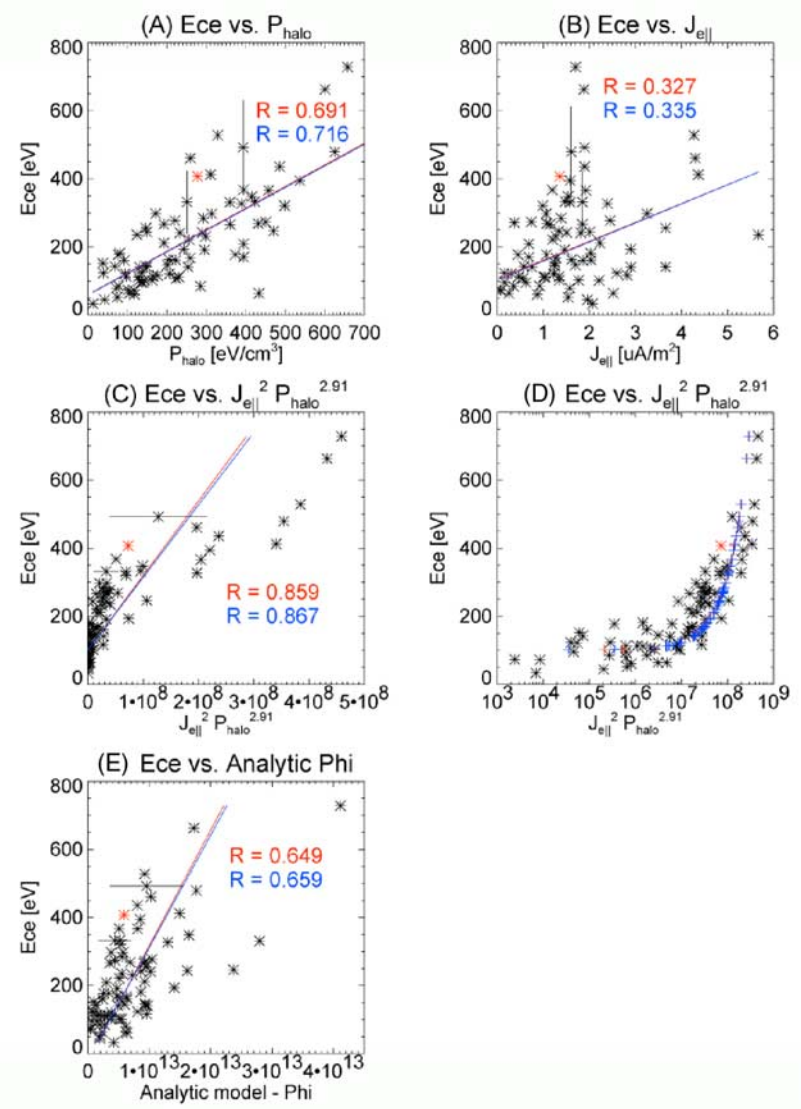

Figure 8. The magnitude of the potential drop as a function of (a) halo pressure, (b) the measured downward field-aligned current from electron moments, (c) the product $\mathbf{J_{e\|}^2 \times P_{halo}^{2.91}}$, (d) the same plot as Figure 8c in log scale on x axis, and (e) the analytic net potential drop along the downward current region flux tube based on *Cran-McGreehin and Wright* [2005a, 2005b]. Each point corresponds to the averaged value per each event.

with the previous observational report (Andersson et al., submitted manuscript, 2007) and numerical study (Newman et al., submitted manuscript, 2007). In these studies, a "no halo" event enhances the possibility of the breakup and reformation state of DCR double layers, which seems to be coincident with earlier stages of the formation of composite potentials in the proposed evolutionary scenario [*Hwang et al.*, 2006b] where halo electrons are often observed to be absent or insignificant. During this stage intermittent signatures of accelerated ionospheric particle moments reported in our companion paper [*Hwang et al.*, 2009] could be caused by these breakup and reformation processes. A halo event enhancing the probability of a stable state of double layers could correspond to the later stage in potential evolution (i.e., U-shaped potentials), in which more fully developed turbulent signatures are observed as shown in our companion paper.

[31] However, the quantitative correlation between halo electron presence and the stability of the potential drop is not as clearly found in our statistics as is the relation between plasma sheet–origin ions and the variability of potential. This discrepancy is resolved by the observation of a positive correlation between the pressures of halo electrons and hot ions that are usually observed together. This means that the correspondence between the two magnetospheric populations makes it appear that halo electrons regulate the fluctuations of the potential magnitudes. However, it seems that heavy ions instead play the main role in reducing the variability of the potential drop, possibly by acting as a sink or buffer for a free energy from the energetic upward electron beams, which otherwise can feed instabilities. The exact mechanism for how the background hot ions of plasma sheet origin can affect the DL and its stability has not been investigated. On the basis of these results from

FAST observations, a numerical study using a Vlasov self-consistent code is to be carried out to enhance our understanding the mechanism of the effects of the plasma sheet ions on the stabilization of the parallel potential drop.

[32] Next, it is found that the magnitude of the potential drop increases with plasma sheet halo electron pressure within each event, and that there is a weak positive correlation between the measured current density and the magnitude of potential drop among U-shaped events. The product of the current density and halo pressure in the form $\mathbf{J}_{\mathbf{e}\|}^{\mathbf{2}} \times \mathbf{P}_{\mathbf{halo}}^{\mathbf{2.91}}$ shows a better correlation to $\epsilon_{\mathbf{ce}}$ than each separate contribution, consequently giving a preliminary empirical current-voltage relation in the downward current region, though other control factors are yet to be found. For instance, ion density may also play a role, as found by *Lynch et al.* [2002].

[33] At least up to FAST altitudes, halo electron pressure is observed to determine the magnitude of potential drop more significantly than the downward current density, that is, with a higher power than that of the current density. The magnetospheric electron contribution to the downward current region IV relation has earlier been predicted by *Temerin and Carlson* [1998]. They suggested that parallel electric fields of downward U-shaped potentials reflect some of the plasma sheet electrons to allow room for the ionospheric electrons, in addition to accelerating the ionospheric electrons by charge neutrality requirements throughout regions along the magnetic field. Therefore, the magnitude of potential drop would be highly dependent on the plasma sheet electrons, and our statistical result indicates that the existence of higher magnetospheric electron pressure is related to the existence of a higher potential drop, which reflects more precipitating plasma sheet electrons, making more room for the upgoing ionospheric electrons.

6. Summary and Future Work

[34] Following our companion paper *Hwang et al.* [2009], which investigated parallel particle signatures in downward current regions associated with the ionospheric-field constraints, we investigate the effect of background plasma sheet conditions on the downward current region potential structures.

[35] 1. Halo electron events are more commonly found in U-shaped potential structures while hot ion events are common for both U-shaped and composite cases.

[36] 2. Halo electrons are observed to partially control the magnitude of the potential drop. This observation can be explained by charge neutrality requirements throughout ionospheric and magnetospheric regions along the magnetic field. This is consistent with the prediction by *Temerin and Carlson* [1998] and analytic and numerical efforts by *Cran-McGreehin and Wright* [2005a, 2005b].

[37] 3. Hot ions are observed to play an important role in reducing the variability of the potential drop. This may be caused by the hot ions acting as a sink or buffer for free energy caused by energetic upward electron beams.

[38] 4. Analysis of current-voltage relations for U-shaped events suggests that the magnitude of DCR potential drop is controlled partially by a combined product of the downward current density from electron moments and plasma sheet halo pressure.

[39] From these statistical studies of background boundary conditions in the auroral downward current region, ionospheric and magnetospheric parameters appear to work together in regulating the resultant potential structures observed at FAST altitudes. The formation of the potential drop or its generation altitude may be critically determined by the local flux-tube conditions in the lower ionosphere, but with restrictions from the magnetospheric conditions such as the downward current density or total parallel potential drop imposed along the flux tube.

[40] A self-consistent simulation will help us understand how background conditions interact with the DCR potential structures. The parameter studies introduced in this and the companion paper will be used to constrain long-range altitude simulations of the microphysics of DCR potential-drop formation and evolution in the context of the larger environment.

[41] **Acknowledgments.** This work was supported by NASA grant NAG5-10472 and by Dartmouth College.

[42] Amitava Bhattacharjee thanks Michael Temerin and another reviewer for their assistance in evaluating this paper.

References

Andersson, L. (2002), Characteristics of parallel electric fields in the downward current region of the aurora, *Phys. Plasmas*, *9*, 3600.

Carlson, C.W., et al. (1998), FAST observations in the downward auroral current region: Energetic upgoing electron beams, parallel potential drops, and ion heating, *Geophys. Res. Lett.*, *25*, 2017.

Cran-McGreehin, A. P., and A. N. Wright (2005a), Electron acceleration in downward auroral field-aligned currents, *J. Geophys. Res.*, *110*, A10S15, doi:10.1029/2004JA010898.

Cran-McGreehin, A. P., and A. N. Wright (2005b), Current-voltage relationship in downward field-aligned current region, *J. Geophys. Res.*, *110*, A10S10, doi:10.1029/2004JA010870.

Ergun, R. (2003), Double layers in the downward current region of the aurora, *Nonlinear Processes Geophys.*, *10*, 45.

Hwang, K.-J., K. Lynch, C. Carlson, J. Bonnell, and W. Peria (2006a), FAST observations of perpendicular DC electric field structures in downward auroral current regions: Morphology, *J. Geophys. Res.*, *111*, A09205, doi:10.1029/2005JA011471.

Hwang, K.-J., K. Lynch, C. Carlson, J. Bonnell, and W. Peria (2006b), FAST observations of perpendicular DC electric field structures in downward auroral current regions: Implication, *J. Geophys. Res.*, *111*, A09206, doi:10.1029/2005JA011472.

Hwang, K.-J., K.A. Lynch, D.L. Newman, and C.W. Carlson (2009), FAST observations of downward current regions: Effect of ionospheric constraints on parallel signatures, *J. Geophys. Res.*, *114*, A02219, doi:10.1029/2008JA013080.

Lynch, K. A., J. W. Bonnell, C. W. Carlson, and W. J. Peria (2002), Return current region aurora: $E_{\|}$, j_z, particle energization and BBELF wave activity, *J. Geophys. Res.*, *107*(A7), 1115, doi:10.1029/2001JA900134.

Marklund, G. T., et al. (2001), Temporal evolution of acceleration structures in the auroral return current region, *Nature*, *414*, 724–727.

McFadden, J. P., C. Carlson, R. Ergun, D. Klumpar, and E. Moebius (1999), Ion and electron characteristics in auroral density cavities associated with ion beams: No evidence for cold ionospheric plasma, *J. Geophys. Res.*, *104*, 14,671.

Temerin, M., and C. W. Carlson (1998), Current-voltage relationship in the downward auroral current region, *Geophys. Res. Lett.*, *25*, 2365.

C. W. Carlson, Space Sciences Laboratory, University of California, Berkeley, CA 94720, USA. (cwc@ssl.berkeley.edu)

K.-J. Hwang, NASA Goddard Space Flight Center, Greenbelt, MD 20771, USA. (joohwang@umbc.edu)

K. A. Lynch, Department of Physics and Astronomy, Dartmouth College, Hanover, NH 03747, USA. (kristina.lynch@dartmouth.edu)

D. L. Newman, Center for Integrated Plasma Studies, University of Colorado, Boulder, CO 80309, USA. (david.newman@colorado.edu)